Available online www.jsaer.com

***Journal of Scientific and Engineering Research*, 2017, 4(10):114-124**

Research Article

ISSN: 2394-2630
CODEN(USA): JSERBR

Lap-shear failure modes of aluminum alloy sheets 2024-T3 welded with friction stir spot FSSW in lower rotational speed and higher dwell time

Karoui MF[1], Souissi R[1], Ayadi M[2]

[1]URMSSDT, ESSTT, University of Tunis,5 Avenue Taha Hussein,BP,56, Bâb Manara 1008,Tunisia
[2]Higher School of Sciences and Techniques of Tunis, Tunisia

Abstract The main FSSW overlapped process parameters focused in this study: plunge rate (0.133, 0.366, and 0.45) mm/s, higher dwell time (5, 10 and 15) s and lower rotational speed (653, 1280 and 1700) tr/mn. Friction stir spot welding aluminum alloy sheet 2024-T3 with 1.6 mm thickness was the aim. Specimen's lap-shear tests were realized to describe how failure mode was developed in the interface joint. In the present work, two fracture modes was investigated, the total pull out nugget failure mode and the mixed pull out- shear nugget failure mode. In two types under lap shear loading conditions, failure initiated by destruction of ZAT, in the first mode the failure propagates continued along joint surface to pull out the total circumference nugget formed by the ZATM and SZ. In second failure mode failure propagates along joint surface to pull out firstly the front mi-circumference nugget near front lower sheet surface; and continued to shear the rest circumference nugget.
The multiple regressions, the pull out nugget and the pull-out-shear nugget, the micro-hardness profile of the welds exhibited a W-shaped appearance and the minimum hardness was measured in the heated affected zone.

Keywords Lap-shear, failure modes, aluminum alloy sheets 2024-T3, FSSW

1. Introduction

1.1. Friction Stir Spot Welding (FSSW)

Friction Stir Spot Welding process (FSSW) was developed in 1991 and has been studied in much applications especially in aeronautic industry [1]. This welding process derives from Friction Stir Welding (FSW), and the main difference is the nugget which formed in circumference joint. Shoulder and pine were the principal entities in friction stir welding tool and the machine use must generate rotation and translation. The main roles of the FSSW tools are to heat the workpiece, induce material flow and constrain the heated metal beneath the tool shoulder and probe friction with the workpiece and by the severe plastic metal deformation. Stirring causes material flow around the probe [2].

In FSSW process, sheets form a lap-joint and the tool penetrates into sheets only in a point, making a punctual bond. The resulting weld has a characteristic hole in the middle of the joint; this hole is left by the probe after removal [3]. In the FSW process sheets are disposed in a butt joint configuration and immobilized to eliminate any displacement when welding process started and tool moves towards the joint direction. Therefore, FSSW process has three steps: plunging, stirring and retracting [4]. Mainly parameters studied are plunge rate, rotational speed, plunge depth, axial load and dwell time [5,6].Analyze of variance pick up correlations between mechanical properties and parameters to find better one to join 2024-T3 aluminum alloy sheets and to understand the influence of each parameters on welds. The mechanical properties measured in most works are restricted to tensile shear tests [5, 7, 8], cross-tension tests [9] and fatigue tests. Some authors have performed studies in AA 5000 and AA 6000 aluminum alloys series, determining fatigue lives, failure modes, micro structural analysis and failure prediction model [10-11]. Different tool geometries have been used, especially

shoulder surface and probe form. Flat, concave, convex, flat with domes, flat with flutes etc... Everyone can be used in shoulder geometry. Cylindrical, conical, triangular, cylindrical threaded, conical threaded, cylindrical fluted etc.., and everyone can be used in probe geometry [12].

In this experimental study, tool geometry and high alloy steel material were kept constant through all experiments. We purpose to screen the effects of three operating factors; tool rotational speed *N*, tool welding rate *V* and dwell time *t.* A conventional experimental procedure was followed to investigate the efficiency of FSSW process parameters, varying one parameter at a time while keeping the other parameters constant. A centered full design with 27 tests was used to realize welding tests to find out the effect of the main process parameters.

To determine mechanical behavior, aluminum alloy 2024-T3 specimens welded with FSSW process was examined in tensile-shear tests on a tensile machine witch unregisters load-elongation response.

The strategy is to use these responses to pick out the failure-shear strength, failure load, plastic rigidity and failure energy used. Then with analysis of variance (ANOVA), provided by multiple regression modeling, coefficient of determination (R^2) and adjusted coefficient of determination (Radj2) are used to select the adequacy models [13].

2. Experimental Procedure

2.1. Welding Process

A.A 2024-T3 aluminum alloy sheet with 1.6 mm thickness was chosen for the present study. His chemical compositions [13] and mechanical properties [14] are listed in Table1 and Table2. AA 2024-T3 a type aluminum alloy belonging to Al-Cu 2000 series. This alloy has good corrosion resistance and weldability and has been widely used in planes.

Table 1: Chemical composition of 2024-T3 aluminum alloys (wt%)

Composant	AL	Cr	Cu	Fe	Mg	Mn	Si	Ti	Zn	auther, each	auther each
Min	90.7	0.1	3.8	0.5	1.2	0.3	0.5	0.15	0.25	0.05	0.15
Max	94.7		4.9		1.8	0.9					

Table 2: Mechanical properties of aluminum alloy 2024-T3

Ultimate tensile strength/ (MPa)	Yield Strength (MPa)	Elongation (%)	Vickers hardness
476	344	17	138

The modifications of micro structural features (material flow, microstructure, stir zone (SZ) size, etc.) and of the internal mechanical state (residual stresses) induced by these different processing configurations.

The lap-shear specimens were made by using two 20 mm x 80 mm x 1.6 mm aluminum sheets with a 20 mm x 30 mm overlap area Fig.1.

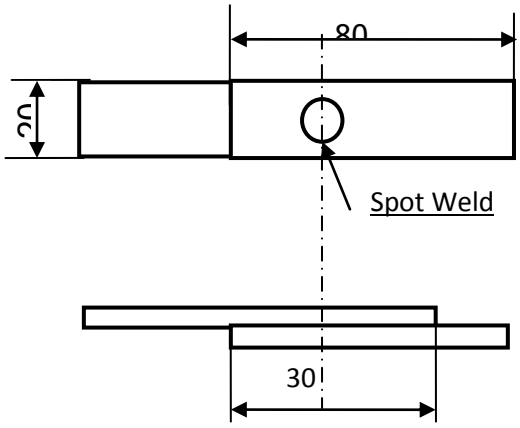

Figure 1: Geometric Dimensions specimen

Weld point made in the overlap area middle with a spot friction by the concave tool. Two square doublers of 20 mm x 30 mm made of aluminum 2024-T3 sheets are located into end sheets and the machine jaws. The doublers are used to align the applied load to avoid the initial realignment of the specimen under lap-shear loading conditions. With fixed probe plunge and shoulder penetration depths 0.2 mm for all tests friction stir

spot welding was realized in same position on overlap area. The welding experiments were conducted in Jendouba Institute of technology (Tunisia), using a conventional vertical milling machine powered 7.5 kW (Momac model), which arranged with a vertical position controlling system. Only the rotational speed N, the plunge rate V and the dwell time t were varied. The welding tool was constituted of high steel Z160CDV12 treated at 62 HRC Table 3, with a conical pin and concave shoulder. The diameter of the shoulder, root and tip of the pin are 10, 4.2 and 3 mm. The pin length is 2.8 mm. And the concave face of the shoulder is angled at 10° Fig.2.

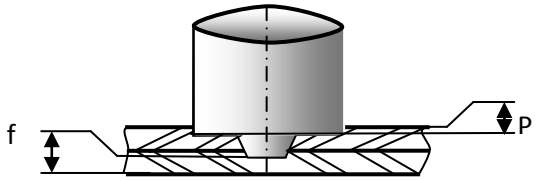

Figure 2: Configuration of shoulder and pin plunge depth

Table 3: Chemical Composition of X160CDV12

Composant	C %	Cr %	SI %	MN%	P%	S%	Mo%	V%
Min	1.45	11	0.1	0.15	0.025 Max	0.025 Max	0.7	0.7
Max	1.7	13	0.4	0.45			1	1

Preliminary welding tests were performed to identify three levels of each factor. They are fixed from visual inspection based on morphology external. The tool rotational speeds, the plunge rates and tool dwell times were varied, which were 653, 1280 and 1700 rpm, 0.133, 0.366, and 0.45 mm/s and 5, 10 and 15 s, respectively. In all cases, the shoulder and tool tip plunge depths (*p,f)* were kept constant 0.2 mm Fig.3.)

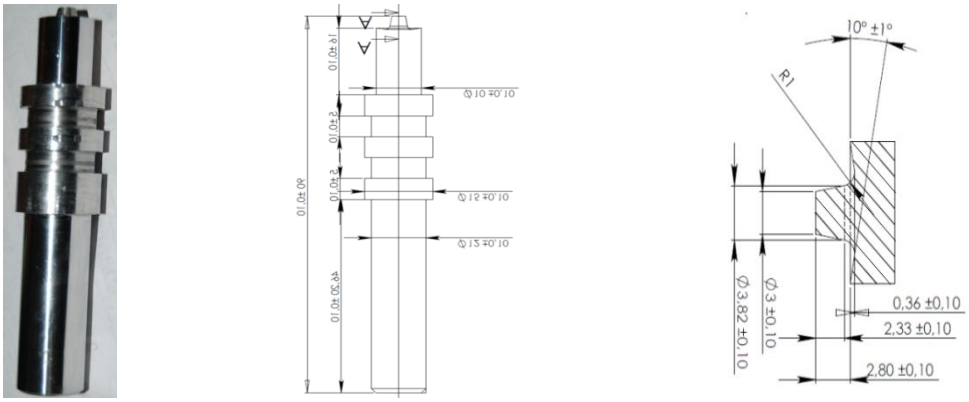

Figure 3: FSSW tool geometry in (mm)

Table 4: Levels for operating parameters for FSW process

Levels	Rotational speed N(Rpm)	Plunge rate V (mm/s)	Dwell time t(s)
Low level	1	1	1
Center level	2,6794	2,4745	2
High level	3	3	3

The experimental layout for three welding parameters with three levels is using a full factorial design with 27 runs. Levels rotational speed and plunge rate two factors aren't symmetric, so the coded values are corrected Table 5.

Figure 4: The universal type tensile testmachineETI-E0015

The lap-shear tensile tests were carried out at 20 °C room temperature, by a universal type tensile test machine as shown in Fig. 4.and were performed for selected welding conditions to evaluate the mechanical strength of the joints produced in this work.

Table 5: Failure load of tensile shear test

N(rpm)	V(mm/mn)	t(s)	F_r(N)
653	8	5	1556
653	8	10	1609
653	8	15	2082
653	22	5	913
653	22	10	2105
653	22	15	2087
653	27	5	1605
653	27	10	1070
653	27	15	1499
1280	8	5	1488
1280	8	10	2040
1280	8	15	1396
1280	22	5	1379
1280	22	10	1882
1280	22	15	1292
1280	27	5	698
1280	27	10	1777
1280	27	15	2497
1700	8	5	718
1700	8	10	1752
1700	8	15	1129
1700	22	5	956
1700	22	10	1079
1700	22	15	1451
1700	27	5	613
1700	27	10	1523
1700	27	15	1685

2.2. Tensile-shear tests

The tensile-shear tests are performed on a testometric's universal testing machines ETI-E0015-200 kN with 0.25 N sensibility. Lap-shear specimens were used to investigate the mechanical behavior of spot friction welds under shear dominant loading conditionsFig.5.Note that the doublers as a rule are used to align the applied load. However, with doublers the rotation nugget persisted still after failure, so clearly in Fig (6d) there is effect of nugget rotation proved by a button appearance on the superior sheet lower face.

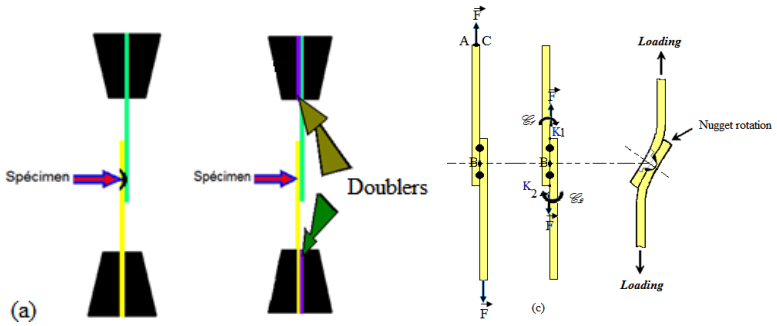

Figure 5: Causes of nuggetrotation (a) Specimen with not doublers, (b) with doublers, (c) nugget rotation in dynamic loading.

The tests were terminated when specimens separated. The load and displacement were simultaneously recorded during the testing. Fig.6 shows a typical load–displacement curve of a spot friction weld made by the concave tool under lap-shear loading conditions.

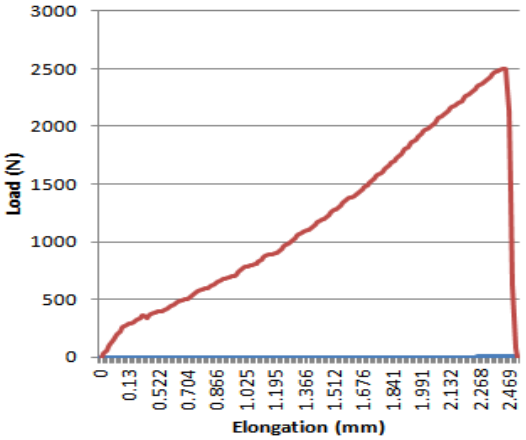

Figure 6: a typical load–displacement curve of a spot friction weld made by the concave tool under lap-shear loading conditions

The nonlinear character of these different dissipation forms can justify research for nonlinear prediction models whose accuracy generally depends on the It can be seen in Table.5 that the average failure load for the specimens tested is 1.48kN. The best performing sample was the sample with 27 mm/min welding feed rate and a 1280 rpm of tool rotating speed with 15s dwell time which achieved 2.49kN. The worst performing sample which has welding parameter 27 mm/min, 1700 rpm and 5s dwell time which only achieved 61.3kN. Two failure spot welds modes are registered will explain later; partially shear mode and totally pullout mode.

3. Response results

3.1. Development of mathematical models

While Friction stir spot welding process is very simple, it involves complex phenomena related to thermo-mechanical and metallurgical transformation in the welded zone. It is generated by converting mechanical energy provided by FSSW and transformed into other types of energy such a sheat, plastic deformation and micro structural transformations.

In order to determine models, relating responses to welding parameters, we chose STATGRAPHICS application which is helpful in developing a suitable approximation for the true functional relationships between quantitative factors (x_1, x_2,., x_k) and the response functions Y= (F_r, K_p, τ_r, E_r) that may characterize the nature of the welded joints as follows:

$Y = f(x_1, x_2, \ldots, x_k) + er$ (1)

The residual error term (er) measures the experimental errors. Such relationship was developed as quadratic polynomial under multiple regression form:

$$Y = b_0 + \sum b_i x_i + \sum b_{ii} x_i^2 + \sum b_{ij} x_i . x_j + er \quad (2)$$

Where b_0 is the average of response; b_i, b_{ii}, and b_{ij} represent regression coefficients. For the three factors, the selected polynomial could be expressed as:

$Y(\tau_r, Frup, Kp, E) = b_0 + b_1.N + b_2.V + b_3.t + b_{11}.N^2 + b_{22}.V^2 + b_{33}.t^2 + b_{12}.N.V + b_{13}.N.t + b_{23}.V.t$ (3)

τ_r = *Failure shear strength; Fr = Failure load;*

Kp= plastic rigidity; Er= failure energy.

The analysis of variance (ANOVA) test was performed to identify the welding parameters that are statistically significant. The purpose of the ANOVA test is to investigate the significance of the welding parameters which affect the failure load, shear strength, plastic rigidity and failure energy of FSSW welds.

3.2. Experimental Responses

To compare results, responses FSSW must be determined from load-displacement curve, nugget geometry and with mathematic relations:

- Shear strength is calculate with two relations:
  - If nugget is completely extract or pull out [14] from upper sheet, so relation (4) must be used.

$$\tau_r = \frac{4.Fr}{\pi(D_e^2 - D_i^2)} \quad (4)$$

Figure 7: Indication of De and Di nugget

  - If an angular sector nugget is partially extract from upper sheet and the rest boundary is sheared, last relation will be changed:

$$\tau_r = \frac{4.Fr}{\alpha.(D_e^2 - D_i^2)} \quad (5)$$

After analysis of the geometry of the welded joint it is noticed that it is divided into two zones, a zone welded by heating effect represented by the stuck diameter (D_c), and another zone welded by thermo mechanical effect defined by the diameter (D_f).

Figure 8: Indication of angular shear nugget

- Failure load and plastic rigidity are determined from load- elongation curve.

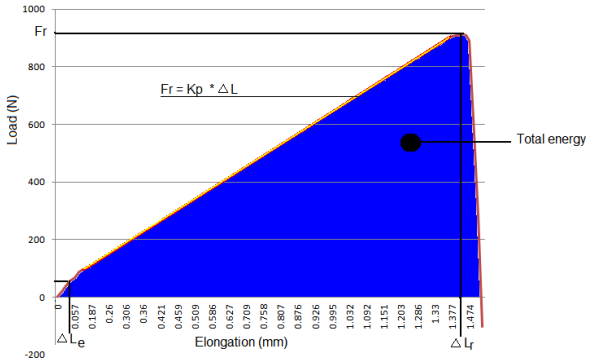

Figure 9: Load-displacement curve

- Failure energy is calculate with relation:

$$E_r = \frac{F_r^2}{2 * Kp} \quad (6)$$

3.3. Factors Effects

- **On lap-shear failure load**

In this study, the tool rotational speed (N) and dwell time (t) are a highly significant factor and play a major role in affecting the lap-shear failure load (LSFL) of the weld as shown in Fig. 10.

- **On shear strength**

In this study, the tool rotational speed (N) is the highly significant factor and plays a major role in affecting the shear strength of the weld as shown in Fig. 10.

- **On plastic rigidity**

In this study, dwell time (t) and the tool rotational speed (N) are a highly significant factor and play a major role in affecting the plastic rigidity (Kp) of the weld as shown in Fig. 10.

- **On failure energy**

In this study, dwell time (t) is a highly significant factor and plays a major role in affecting the failure energy(Er) of the weld as shown in Fig. 10.

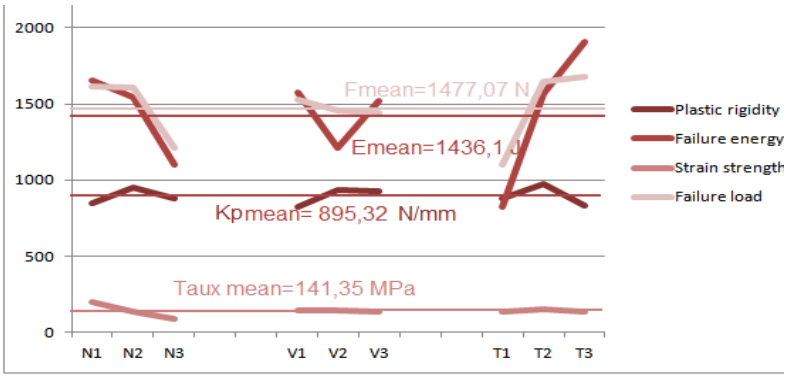

Figure 10: Factors effects on different responses.

3.4. Multiple Regressions

Table.6.lists regression models relating different responses to welding parameters. All selected parameters (N, V, t) for F_r, τ_r, K_p and E_r are statistically significant (P-value less than 0.05) at the 95% confidence level.

However, for the response Fr the parameters N and t have a P-value $<10^{-4}$ and P-value=0.0008 respectively. Consequently, the parameters N, N*N, t, and t*t kept in the model which is nonlinear one.

For the response τ_r the parameters N and t have a P-value $<10^{-4}$ and P-value=0.0129 respectively. Consequently, the parameters N, N*N, t, and t*t kept in the model which is nonlinear one.

For the response K_p the parameters N and t have a P-value $<10^{-4}$ and P-value=0.0170 respectively. Consequently, the parameters N, N*N and V*V kept in the model which is nonlinear one.

For the response K_p the parameters N, t and V have a P-value$<10^{-,4}$, P-value=0.0005and0.0014 respectively. Consequently, the parameters N, N*N, V*t and 1/V kept in the model which is nonlinear one.

Table.6 indicates the adjusted $\boldsymbol{R^2}$statistic of F_r, τ_r, K_p and E_r.

3.5. Average of the differences between the different experimental responses and that calculated

Every X response is calculated with the following relation:

$$\xi\% = \left(\frac{1}{n} \sum \left(\left| \frac{X_{\exp} - X_{calc}}{\tau_{\exp}} \right| \right) \right) * 100$$

Table 6 indicates different averages of the differences between experimental values and that calculate.

4. Joint Performance

Shear fracture of the nugget is observed under tensile/shear loading, which is different from the previous studies [14-19]. These studies indicate that the failure mode is a full nugget pull-out behavior. This failure mode is associated to the combination of process parameters able to produce high resistance welds. In Fig. 11(a, b) lap

shear test results, two failure modes are depicted after investigate and looking for all samples welded in conditions for this work.

4.1. Pull Out Nugget Mode

Typical failed test samples are shown in Fig.8. In the as-welded condition some joints failed by destruction of the area defined by stuck diameter then total wrenching of welded nugget will be take place Fig.11. a. The failure load values unregistered for specimen's number 19, 20, 21and 24, were between 145.1 daN and 71.8 daN.

4.2. Pull Out-shear Nugget Mode

The second mode is the mixed wrenching mode, in which stuck area completely destroyed, then total wrenching nugget affects the front half rings of lower sheet and continuous to shear the remainder of the nugget circle Fig.11.b. The failure load values unregistered on the rest of specimens were between 250 daN and 61.3 daN.

Table 6: Models relating responses to welding parameters

Differential effects of factors on	Size	Factors more influencing	Optimal combination	Model with multiple regression	(1-α)%	R^2%	ξ%
	τ_{max}	*N*	N1, V1 et t2	$Log(\tau_{Cisaillement}) = 5.2123 *N + 1.4907*t - 1.4134*N*N - 0.35152*t*t$	95	99,525	28,13
	F_{max}	*t, N*	N1, V1 et t3	$Log(F_r) = 4,1979*N + 1,8593*t - 1,0964*N*N - 0,39887*t*t$	95	99,611	26,99
	K_p	*t, N*	N2, V2 et t2	$Log(K_p) = 6,9482*N - 1,6334*N*N + 0,08232*V*V$	95	99,422	52,57
	E_{rup}	*t, N*	N1, V1 et t3	$Log(E_{rup}) = 6,5271*N + 2,0441*1/V - 1,7226*N*N + 0,26662*V*t$	95	99,19	55,34

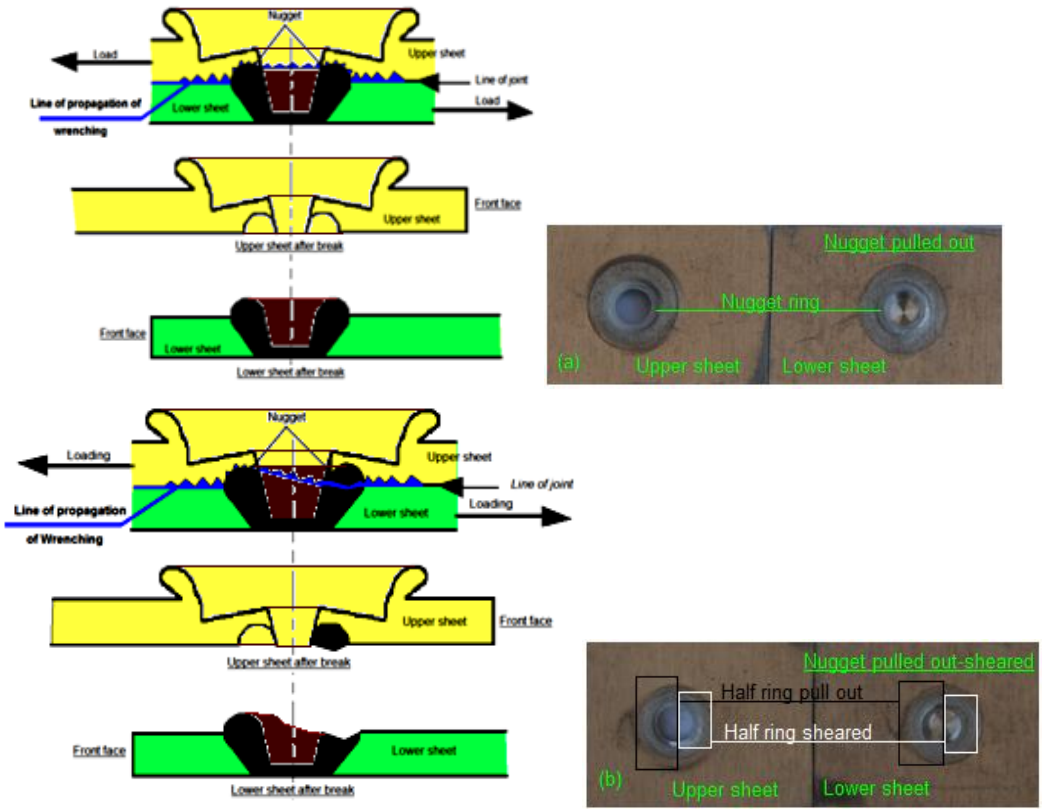

Figure 11: Failure modes (a) Nugget pull out, (b) pull out-shear nugget

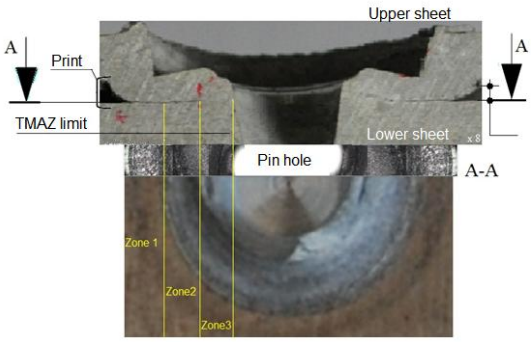

Figure 12: Correspondence of the various zones between a transverse section of a welded point and sight of surface intermediate

4.3. Welded Joint Design

Specimen 18 was crossed in the middle welded point. Common welded lower sheet surface observed in microscope and photographed.

Last three sights were superposed to identify the various zones. Different zones and area were clearly observed, indicating that there is variation in temperature since the pin towards the outside of under shoulder:

Zone 1: thermally affected zone is not really under the shoulder it showed the HAZ. Diameter at this zone is the same of the shoulder's. Even it can be a little largerFig.13**.**

Zone 2: thermally affected zone is really under the shoulder.

Zone 3: thermo mechanically affected zone composed by the TMAZ and SZ, which clearly dissociate fig.14. SZ and TMAZ Thiknesses for specimen 18 were measured. Respectively 0.039 mm and 0.456 mm were the muserments.

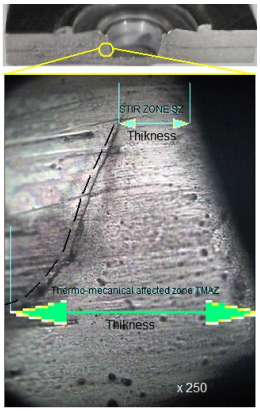

Figure 13: The thermo mechanically affected zone and stir zone

4.4. Hardness Test

The Vickers hardness profiles at lines 1 and 2 mm from the upper surface of the upper sheet shown in Fig. 15. According to the profile of the Vickers hardness, the distribution of Vickers hardness was found to be symmetric with respect to the center of keyhole of the welds made at all given processing parameters [17]. In general, the Vickers hardness reduces with moving away from the upper surface, and the Vickers hardness profile showed a W-shaped appearance. Fig. 14 indicates that the hardness of the base material is about 150 HV. The hardness of the welds is lower than that of the BM. Vickers hardness reduces gradually in the location of HAZ toward the keyhole, reaching the maximum value of 145 HV in the periphery of the HAZ and TMAZ.

The hardness increases in the zone close on both sides to the axis of the hole TMAZ and SZ, however, which is still lower than that of the BM.

We can see that microharness profile realized on two millimeters line from heat source create by rotation tool is above that of 1 mm. Then hardness increases while moving away from the heat source. Thereafter the increase in heat decreases hardness.

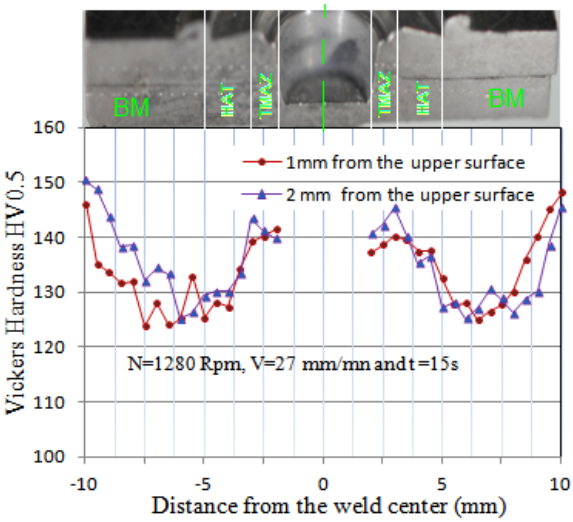

Figure 14: Profile hardness of 1 and 2 mm from the upper surface

Conclusion

Mechanical properties and failure mechanisms of friction stir spot welded 2024-T3 aluminum alloy is investigated based on experimental observations. The following conclusions are made.

- The rotational speed N is a significant factor on mechanical characteristics of the FSSW welded point.
- In conditions to this study; higher failure load, shear stress, plastic rigidity and failure energy will be obtained with 653 and 1280 rotational speeds and 10 and 15s dwell times. And to avoid using the rotational speed 1700 rpm, the plunge rate 27 mm/mn and the dwell time 5s.
- Fig.13, 14 and 15, shows that the architecture of weld point is divided into three regions, BM, HAZ and TMAZ which is combined with SZ identified with layer fine thickness covering the hole left by the probe. Measurements of SZ and TMAZ thicknesses for specimen number 18 by microscope on one side are respectively 0.04 mm and 0.48 mm.
- Remarkable differences of such studies made by several researchers, two failure modes were observed in this study, pull out of the nugget and pull out-shear nugget. The failure load values unregistered were respectively between 145.1 daN, 71.8 daN and 250 daN, 61.3 daN.
- The maximum value of the breaking stress of the first mode, the architecture of different zone and the mode of fracture shows that there is lack of adhesion. Then it is necessary to impose that should not use the conditions of welding which lead to obtaining this mode of fracture.
- In the majority of the cases, the breaking stress increase when increases the speed of rotation and the dwell time.
- The Vickers hardness profile of the sheets showed a W-shaped. The minimum hardness reaches 123 HV in the periphery of the HAZ and TMAZ. Microhardness profile realized on two millimeters line from heat source create by rotational tool is above that of 1 mm. Hardness increases while moving away from the heat source, thereafter the increase in heat decreases hardness.

References

[1]. Thomas W M, Nicholas E D, Needham J C, Murch M G, Temple-Smith P, Dawes C J. Friction stir butt welding, PCT/GB92/ 02203 [P]. 1991.

[2]. R. S. Mishra and M. W. Mahoney: ‘Friction stir welding and processing’; 2007, Materials Park, OH, ASM International.

[3]. Fanelli P, Vivio F, Vullo V. Experimental and numerical characterization of friction stir spot welded joints. Eng Fract Mech 2012; 81:17–25.

[4]. Awang, M.; Mucino, V. H.; Feng, Z.; David S. A. Thermo-Mechanical Modeling of Friction Stir Spot Welding (FSSW) Process: Use of an Explicit Adaptive Meshing Scheme, *2005 SAE International*, 2005-01-1251

[5]. Lathabai, S.; Painter, M.J.; Cantin, G.M.D.; Tyagi, V.K. *Friction spot joining of an extruded Al–Mg–Si alloy.Scripta Materialia* 2006; 55(10):899-902.

[6]. Gerlich, A.; Su, P.; North, T.H.; Bendzsak, G.J. *Friction Stir Spot Welding Of Aluminum and Magnesium Alloys*. Materials Forum 2005;29:290-4.

[7]. Wang, D.-A.; Lee, S.-C. Microstructures and Failure Mechanisms of Friction Stir Spot Welds of Aluminum 6061-T6 Sheets. *Journal of Materials Processing Technology* 2007;186(1-3): 291-7.

[8]. Mitlin, D.; Radmilovic, V.; Pan, T.; Chen, J.; Feng, Z.; Santella, M.L. Structure–properties relations in spot friction welded (also known as friction stir spot welded) 6111 aluminum. *Materials Science and Engineering* 2006;A441:79–96.

[9]. Feng, Z.M.; Santella, L.; David, S.A.; Steel, R.J.; Packer, S.M.; Pan, T. el al. Friction Stir Spot Welding of Advanced High-Strength Steels – A Feasibility Study. *2005 SAE International*, 2005-01-1248.

[10]. Lin, P.-C.; Pan, J.; Pan, T. Failure modes and fatigue life estimations of spot friction welds in lapshear specimens of aluminum 6111-T4sheets. Part 1: Welds made by a concave tool. *International Journal of Fatigue* 2008;30(1):74-89.

[11]. Tran, V.-X.; Pan, J.; Pan, T. Fatigue behavior of aluminum 5754-O and 6111-T4 spot friction welds in lap-shear specimens. *International Journal of Fatigue* 2008;30(12):2175-90.

[12]. Y. N. Zhang, X. Cao, S. Larose and P. *Review of tools for friction stir welding and Processing*. WanjaraCanadian Metallurgical Quarterly 2012 VOL 51 NO 3

[13]. Myers R H, Montgomery D C, Anderson-Cook C M. *Response surface methodology: Process and product optimization using designed experiment [M]*. 3rd Edition. New York: John Wiley & Sons, 2009: 680.

[14]. Jose Antonio Esmerio Mazzaferro, Tonilson de Souza Rosendo, Cintia Cristiane Petry Mazzaferro, Fabiano Dornelles Ramos, Marco Antonio Durlo Tier, Telmo Roberto Strohaecker, Jorge Fernandes dos Santos .*Preliminary Study on the Mechanical Behavior of Friction Spot Welds*. Soldagem Insp. Sao Paulo, Vol. 14, No. 3, p.238-247, Jul/Set 2009.

[15]. Zhang ZH, Yang XQ, Zhang JL, Zhou G, Xu XD, Zou BL. *Effect of welding. Parameters on microstructure and mechanical properties of friction stir spot*. Welded 5052 aluminum alloy. Mater Des 2011;32(8–9):4461–70.

[16]. Tozaki Y, Uematsu Y, Yokaji K. *Effect of welding condition on tensile strength of dissimilar friction stir spot welds between different aluminium alloys*. In: Proceedings of the 6th International Symposium of Friction Stir Welding, Montreal, Canada; October 10–13 2006.

[17]. W. Yuana, R.S. Mishraa, S. Webba, Y.L. Chenb, B.Carlsonb, D.R. Herlingc, G.J. Grantc.*Effect of tool design and process parameters on properties of Al alloy 6016 friction stir spot welds.*Journal of Materials Processing Technology 211 (2011) 972–977.

[18]. Y.C. Chen, S.F. Liu, D. Bakavos, P.B. Prangnell. *The effect of a paint bake treatment on joint performance in friction stir spot welding AA6111-T4 sheet using a pinless tool.* Materials Chemistry and Physics xxx (2013) 1-8.